n-point probability functions for a lattice model of heterogeneous media

Binglin Lu
Department of Mechanical and Aerospace Engineering, North Carolina State University, Raleigh, North Carolina 27695-7910

S. Torquato
Department of Mechanical and Aerospace Engineering and Department of Chemical Engineering, North Carolina State University, Raleigh, North Carolina 27695-7910

(Received 5 April 1990)

The macroscopic properties of two-phase random heterogeneous media depend upon the infinite set of n-point probability functions $S_1, \ldots, S_n$. The quantity $S_n(\mathbf{x}_1, \ldots, \mathbf{x}_n)$ gives the probability of finding n points with positions $\mathbf{x}_1, \ldots, \mathbf{x}_n$ all in one of the phases. We derive a series representation of S_n for a finite-sized D-dimensional lattice model of heterogeneous media. By performing certain averages over the S_n, we then obtain explicit expressions for translationally invariant and rotationally invariant n-point probabilities. Computer simulations are carried out for low-order n-point probability functions. The theoretical and simulation results are found to be in excellent agreement.

I. INTRODUCTION

The quantitative characterization of the microstructure of two-phase random media is not only of importance from a morphological standpoint,[1,2] but also because the macroscopic properties of such materials (transport, mechanical, and electromagnetic properties) depend upon the details of the microstructure.[3–10] The morphology of heterogeneous media can be completely characterized by specifying any of the various infinite sets of statistical correlation functions.[6] One such correlation function is the so-called n-point probability function S_n, which has been shown to arise in rigorous expressions for the conductivity of composites,[3,5,6] fluid permeability of porous media,[7,8] trapping constant associated with diffusion-controlled processes among static traps,[4,9] and the elastic moduli of composites.[10] The quantity $S_n(\mathbf{x}^n)$ (where $\mathbf{x}^n \equiv \mathbf{x}_1, \ldots, \mathbf{x}_n$) gives the probability of finding n points with positions $\mathbf{x}_n$ all in one of the phases, say phase 1. The determination of the $S_n(\mathbf{x}^n)$ in the study of the random media carries the same importance as the determination of the n-particle probability density functions in liquid-state theory.

In the last decade, considerable progress has been made in representing and computing the S_n for off-lattice or continuum models (e.g., distributions of discrete particles).[11–17] Such models are not characterized by *topological equivalence.* A two-phase medium possesses topological equivalence if the morphology at volume fraction ϕ_i is identical to another with volume fraction $1-\phi_i$. Continuum models are useful descriptions of suspensions, beds of particles, particulate composites, etc.

On the other hand, to our knowledge, virtually no work has dealt with the determination and calculation of the S_n for lattice models. The purpose of this paper is to carry out such a program for a simple D-dimensional lattice model that we shall term the "random" lattice model. The random lattice model is constructed by tesselating a D-dimensional cubical subspace into identical D-dimensional cubical cells, with cells randomly and independently designed as phase 1 (white) or phase 2 (black) with probabilities ϕ_1 and ϕ_2, respectively. Thus, our model is essentially the well-known Ising model in the *high-temperature* limit, i.e., the limit in which spin interactions are identically zero. (Note that the random lattice model possesses topological equivalence.) The random lattice model can be profitably used to describe composites with cellular structures, e.g., foams, emulsions, animal and plant tissues, etc. Finally, it should be mentioned that we perform Monte Carlo simulations of certain lower-order S_n in order to confirm our theoretical findings.

In Sec. II we derive a series representation of the S_n for the random lattice model. In Sec. III, we obtain, by performing certain averages over the S_n, translationally invariant and rotationally invariant n-point probabilities. In Sec. IV, the Monte Carlo simulation procedure used to compute lower-order S_n is described. In Sec. V, we graphically display various theoretical results for lower-order n-point probability functions and compare some of these findings to our computer simulation results.

II. SERIES REPRESENTATIONS OF THE S_n FOR THE RANDOM LATTICE MODEL

We shall derive the series representations of the S_n for the random lattice model by employing the corresponding results of Torquato and Stell[11] for the continuum model of distribution of particles. Torquato and Stell expressed the S_n in terms of the n-particle probability density function. Thus our strategy is to exploit the Torquato-Stell results by deriving the n-particle probability density function for the random lattice model. Given the latter, the appropriate expressions of the S_n for the random lattice model easily follow.

 ©1990 The American Physical Society

A. *n*-particle probability density functions

For any statistically inhomogeneous two-phase random medium consisting of identical particles (inclusions) whose positions are completely specified by center-of-mass coordinates $\mathbf{r}^N \equiv \mathbf{r}_1, \ldots, \mathbf{r}_N$, Torquato and Stell[11] derived series representations of the S_n. In the special case of hard particles inclusions, they found that the probability of simultaneously finding n points at positions $\mathbf{x}^n$ all in matrix phase (phase 1, i.e., space exterior to the particles) is given by

$$S_n(\mathbf{x}^n) = 1 + \sum_{k=1}^{n} \frac{(-1)^k}{k!} \int \cdots \int \rho_k(\mathbf{r}^k) \prod_{j=1}^{k} \left\{ 1 - \prod_{i=1}^{n} [1 - m(\mathbf{x}_i - \mathbf{r}_j)] \right\} d\mathbf{r}_j \ , \tag{2.1}$$

where

$$m(\mathbf{x}) = \begin{cases} 1, & \mathbf{x} \in D_P \\ 0, & \text{otherwise} \end{cases} \tag{2.2}$$

is the particle indicator function, $\mathbf{x}$ is a position vector whose origin is the centroid of the particle, and D_P denotes a particle region. The quantity $\rho_n(\mathbf{r}^n)$ in (2.1) is the n-particle probability density function defined by

$$\rho_n(\mathbf{r}^n) = \frac{N!}{(N-n)!} \int P_N(\mathbf{r}^N) d\mathbf{r}_{n+1} \cdots d\mathbf{r}_N \ . \tag{2.3}$$

The n-particle probability density function $\rho_n(\mathbf{r}^n)$ characterizes the probability of simultaneously finding the center of a particle in the volume element $d\mathbf{r}_1$ about $\mathbf{r}_1$, the center of another particle in the volume element $d\mathbf{r}_2$ about $\mathbf{r}_2$, etc. The quantity $P_N(\mathbf{r}^N)$ in (2.3) is the specific N-particle probability density which characterizes the probability of finding the particles labeled $1, 2, \ldots N$ with a particular configuration $\mathbf{r}^N$, respectively.

The task that lies before us is to obtain the appropriate expressions for the $\rho_n(\mathbf{r}^n)$ for the random lattice model, i.e., the lattice problem shall be described in continuum language. Recall that the random lattice model is constructed by tesselating a D-dimensional cubical subspace into M^D identical D-dimensional cubical cells of unit length with cells randomly and independently designated as phase 1 (white) or phase 2 (black) with probabilities ϕ_1 and ϕ_2, respectively (where $\phi_1 + \phi_2 = 1$). Thus the total system volume $V = M^D$. Figure 1 depicts a two-dimensional realization. As noted earlier, the model is closely related to the high-temperature limit of the Ising model. Every cell has two possible states: occupied (black) or unoccupied (white), corresponding to upward or downward spins in the Ising model in high-temperature limit. We let the occupied or black cells correspond to "particles" in the continuum description. Since such cells do not overlap and because multiple occupancy is prohibited then they are regarded as "hard" particles. Let N (where $N \le M^D$) denote the total number of such hard particles (black cells). Then the volume fraction of the black phase $\phi_2 = N/M^D$. Finally, we note that the random lattice model is a special instance of a "symmetric cell material".[18]

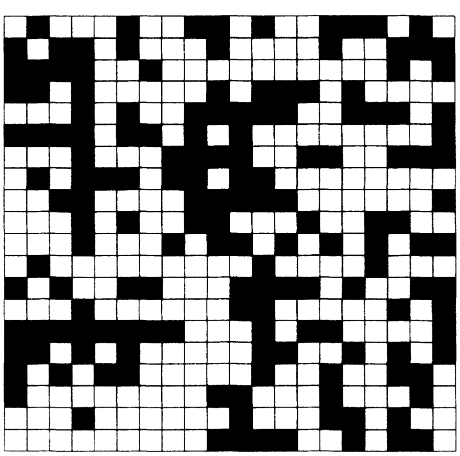

FIG. 1. A two-dimensional realization of the random lattice model at a volume fraction of the black phase $\phi_2 = 0.4$.

For the system described above, the location of a cell is solely determined by the position vector of the cell center which has D components. Specifically, we write the position vector of the jth cell as

$$\mathbf{R}_j = \sum_{k=1}^{D} j_k \mathbf{n}_k \ , \tag{2.4}$$

where $\mathbf{n}_k$ $(k = 1, \ldots, D)$ are the limit vectors in a D-dimensional Cartesian coordinate system. Now the probability of finding a special particle (say particle 1, for example) in a special cell j is just

$$P(\mathbf{r}_1 = \mathbf{R}_j) = \frac{1}{M^D} \prod_{i=2}^{N} \theta(1,i) \tag{2.5}$$

with

$$\theta(1,i) = \begin{cases} 0, & \text{if } \mathbf{r}_1 = \mathbf{r}_i \\ 1, & \text{otherwise} \ . \end{cases} \tag{2.6}$$

The factor on the right-hand side of (2.5) involving $\theta(1,i)$ prevents multiple occupancy of the cell. Thus the N-particle probability density $P_N(\mathbf{r}^N)$ for the random lattice model for $\mathbf{r}^N$ contained within the finite system can be written as

$$P_N(\mathbf{r}^N) = \frac{1}{Z} \prod_{i=1}^{N} \left[\sum_{j=1}^{M^D} \delta(\mathbf{r}_i - \mathbf{R}_j) \right] \prod_{i,j} \theta(i,j) \ , \tag{2.7}$$

where $\delta(\mathbf{x})$ is the Dirac delta function and Z is the normalization constant

$$Z = \int \cdots \int \prod_{i=1}^{N} \left[\sum_{i=1}^{M^D} \delta(\mathbf{r}_i - \mathbf{R}_j) \right] \prod_{i,j} \theta(i,j) d\mathbf{r}^N$$
$$= \frac{M^D!}{(M^D - N)!} \ . \tag{2.8}$$

The n-particle probability density function for the random lattice model can be obtained using (2.3) and (2.7), with the result that

$$\rho_n(\mathbf{r}^n)=\frac{N!}{(N-n)!}\frac{Z_n}{Z}\prod_{i=1}^{n}\left[\sum_{j=1}^{M^D}\delta(\mathbf{r}_i-\mathbf{R}_j)\right]\prod_{i,j}\theta(i,j)\ , \tag{2.9}$$

where

$$Z_n=\frac{(M^D-n)!}{(M^D-N)!}\ . \tag{2.10}$$

It is important to note that the above development for the P_n and ρ_n was limited to positions $\mathbf{r}^N$ located within the finite system. Exterior to the generally finite system, P_n and ρ_n are identically zero.

B. Series expressions for the $S_n(\mathbf{x}^n)$

Substitution of (2.9) into the general series expansion of (2.1) enables one to obtain the n-point probability function S_n for this model. For the random lattice model the indicator function $m(\mathbf{x})$ is given as

$$m(\mathbf{x})=\begin{cases}1, & |x_k|\le\frac{1}{2}\quad(k=1,\dots,D)\\ 0, & \text{otherwise}\ ,\end{cases} \tag{2.11}$$

where $\mathbf{x}$ is measured with respect to the centroid of a cell and x_k is the kth component of $\mathbf{x}$. For $n=1$ and $n=2$ we have the following expressions which apply within the finite system:

$$S_1(\mathbf{x})=1-\int\rho_1(r_1)m(\mathbf{x}-\mathbf{r}_1)d\mathbf{r}_1\ , \tag{2.12}$$

$$\begin{aligned}S_2(\mathbf{x}_1,\mathbf{x}_2)=1&-\int\rho_1(\mathbf{r}_1)m(\mathbf{x}-\mathbf{r}_1)d\mathbf{r}_1\\&-\int\rho_1(\mathbf{r}_1)m(\mathbf{x}_2-\mathbf{r}_1)d\mathbf{r}_1\\&+\int\rho_1(\mathbf{r}_1)m(\mathbf{x}_1-\mathbf{r}_1)m(\mathbf{x}_2-\mathbf{r}_1)d\mathbf{r}_1\\&+\int\rho_2(\mathbf{r}_1,\mathbf{r}_2)m(\mathbf{x}_1-\mathbf{r}_1)m(\mathbf{x}_2-\mathbf{r}_2)d\mathbf{r}_1d\mathbf{r}_2\ .\end{aligned} \tag{2.13}$$

The integral of (2.12) is trivial and leads to the simple result that

$$S_1(\mathbf{x})=1-\phi_2=\phi_1\ , \tag{2.14}$$

where

$$\phi_2=\frac{N}{M^D}=\frac{N}{V} \tag{2.15}$$

is the volume fraction of phase 2. Thus, $S_1(\mathbf{x})$ is equal to the constant ϕ_1 within the system and zero otherwise.

For pairs of points within the system, the two-points probability function varies not only with the relative distance between the two points, but also varies with the locations of the two points. This can be seen from the expression (2.13). When $\mathbf{x}_1$ and $\mathbf{x}_2$ lie *anywhere* in the *same white cell*, we have

$$m(\mathbf{x}_1-\mathbf{r}_1)m(\mathbf{x}_2-\mathbf{r}_1)=1$$

and

$$m(\mathbf{x}_1-\mathbf{r}_1)m(\mathbf{x}_2-\mathbf{r}_2)=0\ .$$

The integration then yields the two-point probability function as

$$S_2^{(1)}(\mathbf{x}_1,\mathbf{x}_2)=1-\phi_2=\phi_1\ . \tag{2.16}$$

The superscript 1 here indicates that the special case of pairs of points lying in the same white cell is being considered. When these two points are both in one white cell, then the two-point probability gives the same result as if these two points coincided. When $\mathbf{x}_1$ and $\mathbf{x}_2$ lie *anywhere* in different white cells, we have

$$m(\mathbf{x}_1-\mathbf{r}_1)m(\mathbf{x}_2-\mathbf{r}_1)=0$$

and

$$m(\mathbf{x}_1-\mathbf{r}_1)m(\mathbf{x}_2-\mathbf{r}_2)=1\ .$$

The integration then leads to a different result:

$$S_2^{(2)}(\mathbf{x}_1,\mathbf{x}_2)=1-2\phi_2+\phi_2\frac{\phi_2-1/M}{1-1/M}\ . \tag{2.17}$$

The superscript 2 here indicates that the special case of pairs of points lying in *different* white cells is being considered. When the two points are in different cells, the probability of finding both points in phase 1 is equal to the probability of finding the two cells unoccupied. Note that in the limit of an infinite system ($M\to\infty$), Eq. (2.17) yields ϕ_1^2. Thus, Eqs. (2.16) and (2.17) imply that the random lattice model is statistically inhomogeneous even in the infinite-system limit. Other examples of infinite but inhomogeneous systems include regular (periodic) lattices.

The general result for the S_n of the random lattice model for any n can be obtained by substituting (2.9) into (2.1). Therefore, we have the general expression

$$S_n^{(l)}(\mathbf{x}_n)=1-\sum_{k=1}^{l}\frac{l!}{k!(l-k)!}\frac{\phi_2(\phi_2-1/M)\dots[\phi_2-(k-1)/M]}{(1-1/M)\dots[1-(k-1)/M]}\ ,\quad l=1,\dots,n\ . \tag{2.18}$$

$S_n^{(l)}$ in (2.18) is the n-point probability function for any partition of n points among l different white cells such that the points lie anywhere in the white cells.

III. TRANSLATIONALLY INVARIANT AND ROTATIONALLY INVARIANT n-POINT PROBABILITY FUNCTIONS

A. Translationally invariant functions

We shall obtain translationally invariant n-point probability functions by fixing the relative displacement between the n points $\mathbf{x}_{12},\dots,\mathbf{x}_{1n}$ (where $\mathbf{x}_{1i}=\mathbf{x}_i-\mathbf{x}_1$) and averaging over the positions $\mathbf{x}_1$. This averaged function, denoted by $\hat{S}_n$, depends upon the aforementioned relative displacements and has the following interpretation: the probability of tossing a polyhedron with *fixed orientation* having n vertices with relative displacements $\mathbf{x}_{12},\dots,\mathbf{x}_{1n}$, anywhere in the two-phase medium and finding the n vertices in the white phase. The general expression for $\hat{S}_n$ can be written in terms of the $S_n^{(l)}$ [Eq. (2.18)] as follows:

$$\hat{S}_n(\mathbf{x}_{12},\ldots,\mathbf{x}_{1n})=\sum_{l=1}^{n}\hat{W}_n^{(l)}(\mathbf{x}_{12},\ldots,\mathbf{x}_{1n})S_n^{(l)} \quad (3.1)$$

with

$$\sum_{1}^{n}\hat{W}_n^{(l)}=1\ , \quad (3.2)$$

where $\hat{W}_n^{(l)}$ is the weight factor associated with the averaging described above. The $\hat{W}_n^{(l)}$ have simple probabilistic interpretations: $\hat{W}_n^{(l)}(\mathbf{x}_{12},\ldots,\mathbf{x}_{1n})$ gives the probability of finding the n vertices of the aforementioned polyhedron of fixed orientation in *any l different* cells (black or white). We now give explicit expressions for $\hat{W}_n^{(l)}$ and $\hat{S}_n$ for the cases of $n=2$ and $n=3$ and for various values of the dimensionality D.

1. Two-point probability function $\hat{S}_2$

We first give $\hat{S}_2$ for $D=1$, 2, and 3. From (3.1), one has

$$\hat{S}_2=\hat{W}_2^{(1)}S_2^{(1)}+\hat{W}_2^{(2)}S_2^{(2)}\ . \quad (3.3)$$

The weight factors are easily derived using geometrical probability arguments. We merely state these results rather than give any details. In the case of $D=1$, we have

$$\hat{W}_2^{(1)}(r)=\begin{cases}1-r, & r\le 1\\ 0, & r>1\end{cases} \quad (3.4)$$

and

$$\hat{W}_2^{(2)}(r)=\begin{cases}r, & r\le 1\\ 1, & r>1\ ,\end{cases} \quad (3.5)$$

where r is the relative distance between the two points. Combination of (2.16), (2.17), and (3.3)–(3.5) then yields for $D=1$ that

$$\hat{S}_2(r)=\begin{cases}(1-r)(1-\phi_2)+r\left[1-2\phi_2+\phi_2\dfrac{\phi_2-1/M}{1-1/M}\right], & r\le 1\ ,\\ 1-2\phi_2+\phi_2\dfrac{\phi_2-1/M}{1-1/M}, & r>1\ .\end{cases} \quad (3.6)$$

For the two-dimensional random lattice model, the weight factors are given by

$$\hat{W}_2^{(1)}(r,\theta)=(1-r\cos\theta)(1-r\sin\theta)H(1-r\cos\theta)\times H(1-r\sin\theta)\ . \quad (3.7)$$

and

$$\hat{W}_2^{(2)}(r,\theta)=1-\hat{W}_2^{(1)}(r,\theta)\ , \quad (3.8)$$

where $H(x)$ is the Heaviside step function and θ is the angle that the vector $\mathbf{r}$ makes with the horizontal. Thus, by (3.1), we have

$$\hat{S}_2(r,\theta)=\hat{W}_2^{(1)}(r,\theta)S_2^{(1)}+\hat{W}_2^{(2)}(r,\theta)S_2^{(2)}\ . \quad (3.9)$$

Note that $\hat{S}_2(r,\theta)$ possesses reflection symmetry about $\theta=\pi/4$.

In the instance of $D=3$, the weight factors are given by the following formulas:

$$\hat{W}_2^{(1)}(r,\theta,\phi)=(1-r\cos\theta)(1-r\sin\theta\sin\phi)(1-r\sin\theta\cos\phi)\times H(1-r\cos\theta)H(1-r\sin\theta\sin\phi)\times H(1-r\sin\theta\cos\phi)\ ,\quad 0\le\theta\le\pi/2,\ \ 0\le\phi\le\pi/2 \quad (3.10)$$

and

$$\hat{W}_2^{(2)}=1-\hat{W}_2^{1}(r,\theta,\phi),\quad 0\le\theta\le\pi/2, 0\le\phi\le\pi/2\ . \quad (3.11)$$

Here θ and ϕ are the spherical polar and azimuthal angles associated with the vector $\mathbf{r}$. Finally, use of (3.1) yields

$$\hat{S}_2(r,\theta,\phi)=\hat{W}_2^{(1)}(r,\theta,\phi)S_2^{(1)}+\hat{W}_2^{(2)}(r,\theta,\phi)S_2^{(2)}\ . \quad (3.12)$$

Because of symmetry, we need only consider the angles θ and ϕ in the range indicated.

2. Three-point probability function $\hat{S}_3$

Calculation of the $\hat{S}_n$ for $n\ge 3$ becomes progressively more complex. Here we shall give the relation for $\hat{S}_3$ in the one-dimensional case only since it can be expressed analytically.

For the case of $D=1$, $\hat{S}_3(r_1,r_2)$ can be evaluated analytically. Here r_1 is the distance between one extreme point and the intermediate point and r_2 is the distance between the other extreme point and the intermediate point. We find that

$$\hat{S}_3(r_1,r_2)=(1-\phi_2)(1-r_1-r_2)+\left[1-2\phi_2+\phi_2\frac{\phi_2-1/M}{1-1/M}\right](r_1+r_2),\quad r_1+r_2<1 \quad (3.13)$$

$$\hat{S}_3(r_1,r_2)=\left[1-2\phi_2+\phi_2\frac{\phi_2-1/M}{1-1/M}\right](2-r_1-r_2)+\left[1-3\phi_2+\frac{3\phi_2(\phi_2-1/M)}{1-1/M}+\frac{\phi_2(\phi_2-1/M)(\phi_2-2/M)}{(1-1/M)(1-2/M)}\right](r_1+r_2-1)\ ,\quad r_1+r_2>1 \text{ and } r_1<1, r_2<1\ , \quad (3.14)$$

$$\hat{S}_3(r_1,r_2)=\left[1-2\phi_2+\phi_2\frac{\phi_2-1/M}{1-1/M}\right](2-r_1-r_2)+\left[1-3\phi_2+\frac{3\phi_2(\phi_2-1/M)}{1-1/M}-\frac{\phi_2(\phi_2-1/M)(\phi_2-2/M)}{(1-1/M)(1-2/M)}\right](r_1+r_2-1)\,,\quad r_1+r_2>1 \text{ and } r_1<1, r_2<1\,, \tag{3.15}$$

$$\hat{S}_3(r_1,r_2)=\left[1-2\phi_2+\phi_2\frac{\phi_2-1/M}{1-1/M}\right](2-r_1-r_2)+\left[1-3\phi_2+\frac{3\phi_2(\phi-1/M)}{1-1/M}-\frac{\phi_2(\phi_2-1/M)(\phi_2-2/M)}{(1-1/M)(1-2/M)}\right](r_1+r_2-1)\,,\quad r_1+r_2>1 \text{ and } r_1<1, r_2<1\,, \tag{3.16}$$

$$\hat{S}_3(r_1,r_2)=1-3\phi_2+\frac{3\phi_2(\phi_2-1/M)}{1-1/M}-\frac{\phi_2(\phi_2-1/M)(\phi_2-2/M)}{(1-1/M)(1-2/M)},\quad r_1>1 \text{ and } r_2>1\,. \tag{3.17}$$

B. Rotationally invariant functions

Here we shall obtain rotationally invariant n-point probability function by averaging the $\hat{S}_n$ obtained above over the $[(D-2)n+1]$ angular coordinates associated with the fixed $(n-1)$ relative distances $x_{12},\ldots,x_{1n}$, where $x_{1i}=|\mathbf{x}_{1i}|$. We denote such an n-point probability function which will depend upon the distances $x_{12},\ldots,x_{1n}$ by $\bar{S}_n$. This can be reinterpreted as the probability of finding the n vertices of a polyhedron separated by the relative distances $x_{12},\ldots,x_{1n}$ in the white phase when tossed, without regard to orientation, into the two-phase medium. The general expression for $\bar{S}_n$ is obtained by averaging (3.1) with the result that

$$\bar{S}_n(x_{12},\ldots,x_{1n})=\sum_{l=1}^{n}\bar{W}_n^{(l)}(x_{12},\ldots,x_{1n})S_n^{(l)} \tag{3.18}$$

with

$$\sum_{1}^{n}\bar{W}_n^{(l)}=1\,, \tag{3.19}$$

where $\bar{W}_n^{(l)}$ is the weight factor associated with the averaging described above. $\bar{W}_n^{(l)}$ has a simple probabilistic interpretation: $\bar{W}_n^{(l)}(x_{12},\ldots,x_{1n})$ gives the probability of finding the n vertices of a polyhedron separated by the relative distances $x_{12},\ldots,x_{1n}$ in *any* l different cells (black and white) when tossed, without regard to orientation, into the two-phase medium. Note that in the case $D=1$, $\hat{S}_n=\bar{S}_n$, i.e., the translationally invariant functions equal the rotationally invariant functions. Thus, the aforementioned results given for the $\hat{S}_2$ and $\hat{S}_3$ for $D=1$ are also corresponding results for $\bar{S}_2$ and $\bar{S}_3$.

We now give explicit expressions for $\bar{W}_2^{(l)}$ and $\bar{S}_2$ for $D=2$ and $D=3$. The quantity $S_2(r)$ for $D=2$ is easily obtained by averaging $\hat{S}_2(r,\theta)$ [Eq. (3.9)] over the angle θ, i.e.,

$$\bar{S}_2(r)=\bar{W}_2^{(1)}(r)S_2^{(1)}+\bar{W}_2^{(2)}(r)S_2^{(2)}\,, \tag{3.20}$$

where

$$\bar{W}_2^{(i)}(r)=\frac{4}{\pi}\int_0^{\pi/4}\hat{W}_2^{(i)}(r,\theta)d\theta,\quad (i=1,2)\,. \tag{3.21}$$

The elementary integrals of (3.19) combined with (3.18) finally yields

$$\bar{S}_2(r)=\frac{\pi}{4}(1-\phi_2)\left[\frac{\pi}{4}\cos^{-1}g(r)-r\{g(r)-[1-g^2(r)]^{1/2}\}+\frac{r^2}{4}[2g^2(r)-1]\right]H(\sqrt{2}-r)+\frac{\pi}{4}\left[1-2\phi_2+\phi_2\frac{\phi_2-1/M}{1-1/M}\right]\times\left[H(r-\sqrt{2})+\left[\cos^{-1}g(r)+r\{g(r)-[1-g^2(r)]^{1/2}\}-\frac{r^2}{4}[2g^2(r)-1]\right]H(\sqrt{2}-r)\right]\,, \tag{3.22}$$

where

$$g(r)=\frac{1}{(r-1)H(r-1)+1}\,. \tag{3.23}$$

In the case $D=3$, the weights $\bar{W}_2^{(i)}(r)$ are obtained by performing the following averages over the $\hat{W}_2^{(i)}(r,\theta,\phi)$ [Eqs. (3.10) and (3.11)]:

$$\bar{W}_2^{(i)}(r)=\frac{2}{\pi}\int_0^{\pi/2}\int_0^{\pi/2}\bar{W}_2^{(i)}(r,\theta,\phi)\sin\theta\, d\theta\, d\phi,\quad (i=1,2)\,. \tag{3.24}$$

The integrals of (3.24) cannot be performed analytically and are thus computed numerically using Simpson's rule. Substitution of (3.24) into (3.20) yields $\bar{S}_2(r)$ for $D=3$.

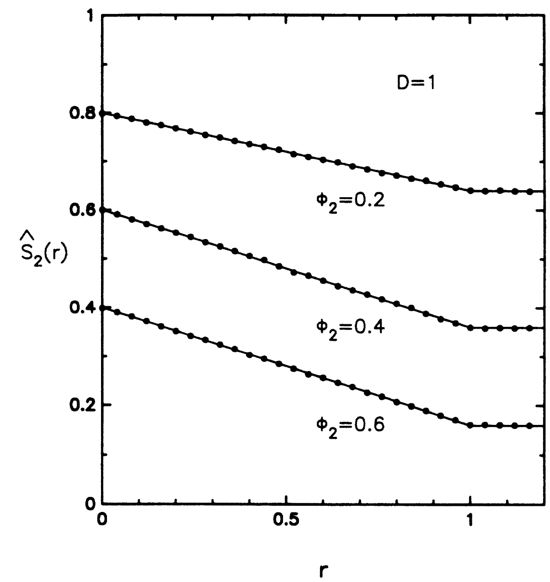

FIG. 2. The translationally invariant two-point probability function $\hat{S}_2(r)$ for $D=1$ at $\phi_2=0.2$, 0.4, and 0.6, respectively. The solid line is the analytical result calculated from (3.6). The circles are the simulation data. Note $\hat{S}_2=\bar{S}_2$ for $D=1$.

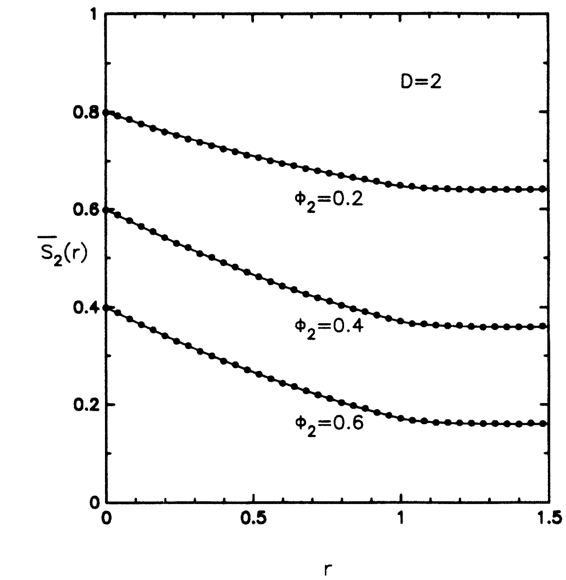

FIG. 4. The rotationally invariant two-point probability function $\bar{S}_2(r)$ for $D=3$ at $\phi_2=0.2$, 0,4, and 0.6, respectively. The solid line is the analytical result calculated from (3.22). The circles are the simulation data.

IV. SIMULATION PROCEDURE

In order to verify our theoretical results, we have performed Monte Carlo simulations to compute the rotationally invariant functions $\bar{S}_2(r)$ for $D=1$, 2, and 3 and $\bar{S}_3$ for $D=1$. Obtaining such measures is a two step process: first, one generates realizations of the medium and second, one samples for the statistical quantities of interest. In all our simulations, M^D, the total number of lattice cells, equaled 10^6. Periodic boundary conditions were employed. The state of a cell (black or white) was determined according to the prescribed probability ϕ_2. In the case $D=1$, $\bar{S}_2(r)$ was then determined by randomly

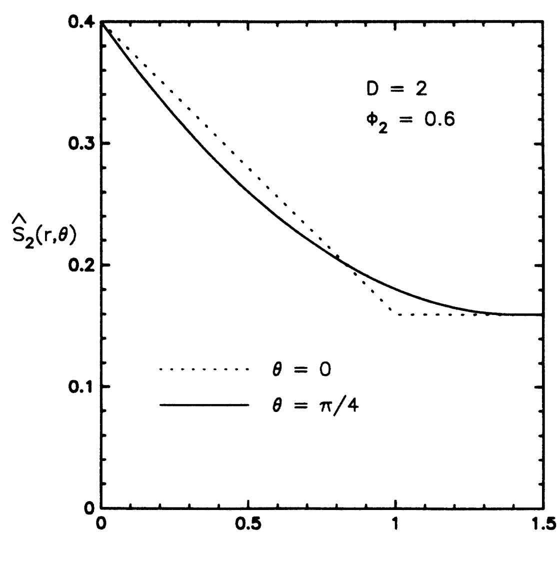

FIG. 3. The translationally invariant two-point probability function $\hat{S}_2(r,\theta)$ for $D=2$ at $\phi_2=0.4$ as computed from (3.9) for two different angles: $\theta=0$ and $\theta=\pi/4$.

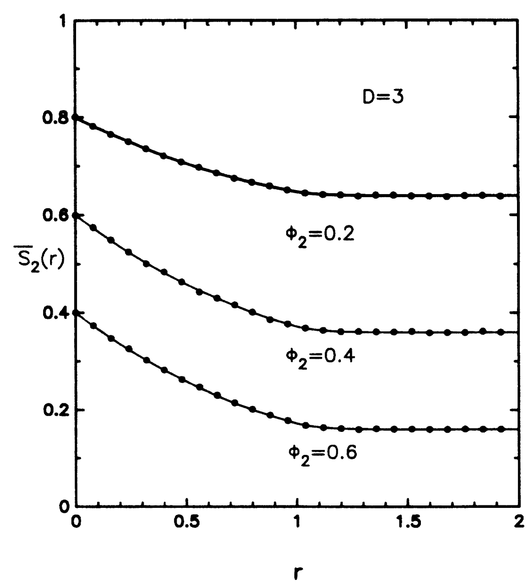

FIG. 5. The rotationally invariant two-point probability function $\bar{S}_2(r)$ for $D=3$, at $\phi_2=0.2$, 0.4, and 0.6, respectively. The solid line is the analytical result calculated from (3.20) and (3.24). The circles are the simulation data.

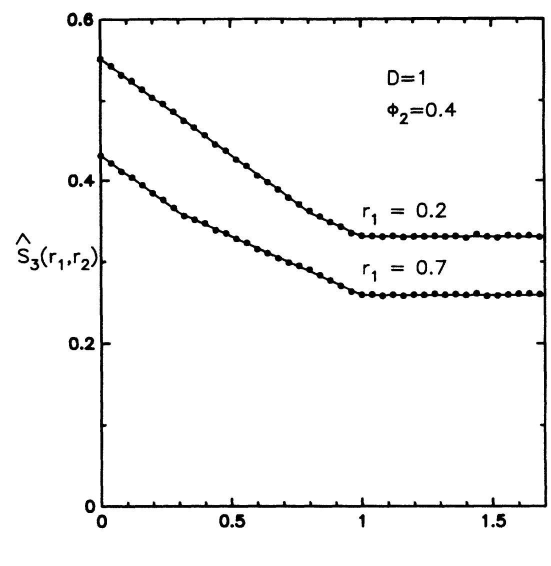

FIG. 6. The translationally invariant three-point probability function $\hat{S}_3(r_1 r_2)$ for $D=1$ at $\phi_2=0.4$ as a function of r_2 for two fixed values of r_1: $r_1=0.2$ and $r_1=0.7$. The solid line is the analytical result calculated from (3.13)–(3.17). The circles are the simulation data. Note $\hat{S}_3=\bar{S}_3$ for $D=1$.

choosing 10^5 initial and end points, each pair of points separated by a distance r. In the instance of $D=2$, we chose 800 initial points and for every initial point, 400 different end points (each at a distance r from the initial point) were randomly chosen. In the case of $D=3$, 100 initial points were randomly chosen, and for every initial point, 5000 end points were randomly chosen. The number of successes (i.e., the number of times both points fall in the white phase) divided by the total number of line segments was recorded to obtain $\bar{S}_2(r)$. For the three-point probability function, we have performed the computer experiment for the simplest case $D=1$ only. Here $\bar{S}_3=\hat{S}_3$ is a function of the relative distances r_1 and r_2 (described above) and the simulation procedure used to obtain it is similar to the one carried out to compute $\bar{S}_2(r)=\hat{S}_2$ for $D=1$.

V. RESULTS

Our theoretical results for lower-order n-point probability functions (given in Sec. III) are graphically displayed in Figs. 2–6. In almost all of these cases, computer simulation data are included. Theoretical results are seen to be in excellent agreement with the data.

In Figs. 2 and 3 we plot $\hat{S}_2$ for $D=1$ and $D=2$, respectively, at selected values of ϕ_2. As noted earlier, for $D=1$, translationally invariant and rotationally invariant n-point probability functions are precisely the same, i.e., $\hat{S}_n=\bar{S}_n$. Figures 4 and 5 depict $\bar{S}_2(r)$ for $D=2$ and $D=3$, respectively, at $\phi_2=0.2$, 0.4, and 0.6. The two-point probability function, in all cases, is a monotonically decreasing function of r until it achieves its long-range value of ϕ_1^2. In contrast to the two-point probability function for $D\geq 2$, the first derivative of $\bar{S}_2(r)=\hat{S}_2(r)$ for $D=1$ is discontinuous at $r=1$ (cell length). The origin of this discontinuity is the term $\bar{W}_2^{(1)}S_2^{(1)}$ in Eq. (3.6). Moreover, unlike $\bar{S}_2(r)$ for $D\geq 2$, $\bar{S}_2(r)$ for $D=1$ is linear in r for $r\leq 1$. Note $\hat{S}_2(r,\theta=0)$ for $D=2$ equals $\hat{S}_2(r)$ for $D=1$ for obvious reasons. Not surprisingly, $\hat{S}_2(r,\theta=\pi/4)$ is a smoother and longer-ranged function. Observe that $\bar{S}_2(r)$ attains its long-range value of ϕ_1^2 for larger values of r as D increases ($r=1$ for $D=1$, $r=\sqrt{2}$ for $D=2$, and $r=\sqrt{3}$ for $D=3$) even though for all D it is numerically close to ϕ_1^2 at $r=1$. Finally we remark that the shape of $\bar{S}_2(r)$ is reminscent of the shape of the two-point probability function for fully penetrable (D-dimensional) spheres.[12]

Figure 6 displays the three-point probability function $\hat{S}_3$ for $D=1$ at $\phi_2=0.4$ as a function or r_2 for the fixed values of r_1:$r_1=0.2$ and $r_1=0.7$. For fixed r_2, the probability of finding three points in the white phase decreases as r_1 increases, as expected. Of course if both r_1 and r_2 are larger than unity, then $\hat{S}_3=\phi_1^3$.

ACKNOWLEDGMENT

This work was supported by the Office of Basic Energy Science, U.S. Department of Energy under Grant No. DE-FG05-86ER13482.

[1]P. Debye and A. M. Bueche, J. Appl. Phys. **20**, 518 (1949).
[2]B. Lu and S. Torquato, J. Opt. Soc. Am. A **7**, 717 (1990).
[3]M. J. Beran, *Statistical Continuum Theories* (Wiley, New York, 1968).
[4]R. A. Reck and S. Prager, J. Chem. Phys. **42**, 3027 (1965).
[5]G. W. Milton, Phys. Rev. Lett. **46**, 542 (1981).
[6]S. Torquato, Rev. Chem. Eng. **4**, 151 (1987).
[7]S. Prager, Phys. Fluids **4**, 1477 (1961); J. G. Berryman and G. W. Milton, J. Chem. Phys. **83**, 754 (1985).
[8]J. Rubinstein and S. Torquato, J. Fluid Mech. **206**, 25 (1989).
[9]J. Rubinstein and S. Torquato, J. Chem. Phys. **88**, 6372 (1988).
[10]G. W. Milton and N. Phan-Thien, Proc. R. Soc. London, Ser. A **380**, 305 (1982).
[11]S. Torquato and G. Stell, J. Chem. Phys. **77**, 2071 (1982).
[12]S. Torquato and G. Stell, J. Chem. Phys. **79**, 1510 (1983).
[13]S. Torquato and G. Stell, J. Chem. Phys. **82**, 980 (1985).
[14]S. Torquato and F. Lado, J. Phys. A **18**, 141 (1985).
[15]S. Torquato and J. D. Beasley, Int. J. Eng. Sci. **24**, 415 (1986); C. G. Joslin and G. Stell, J. Appl. Phys. **60**, 1067 (1986).
[16]G. Stell and P. A. Rikvold, Chem. Eng. Commun. **51**, 233 (1987).
[17]S. Torquato and A. K. Sen, J. Appl. Phys. **67**, 1145 (1990).
[18]M. Miller, J. Math. Phys. **10**, 1988 (1969).